

New lithium-ion conducting perovskite oxides related to (Li, La)TiO₃

LITTY SEBASTIAN, A K SHUKLA and J GOPALAKRISHNAN*
Solid State and Structural Chemistry Unit, Indian Institute of Science,
Bangalore 560 012, India
e-mail: gopal@sscu.iisc.ernet.in

Abstract. We describe the synthesis and lithium-ion conductivity of new perovskite-related oxides of the formulas, $\text{LiCa}_{1.65}\square_{0.35}\text{Ti}_{1.3}\text{B}_{1.7}\text{O}_9$ (B = Nb, Ta) (**I, II**), $\text{LiSr}_2\text{Ti}_{2.5}\text{W}_{0.5}\text{O}_9$ (**III**) and $\text{LiSr}_{1.65}\square_{0.35}\text{Ti}_{2.15}\text{W}_{0.85}\text{O}_9$ (**IV**). Oxides **I** and **II** crystallize in orthorhombic (GdFeO₃-type) structure, while oxides **III** and **IV** possess cubic symmetry. All of them exhibit significant lithium-ion conduction at high temperatures, the highest conductivity of $\sim 10^{-2}$ S/cm at 800°C among the oxides is exhibited by the composition **IV**. The results are discussed in the light of previous work on lithium-ion conducting perovskite oxides containing d^0 cations.

Keywords. Lithium ion conductors; lithium–lanthanum perovskites; lithium–lanthanum titanates.

1. Introduction

There is a continuous search for new materials exhibiting high lithium ion conductivity in view of their potential technological application as solid electrolytes in high energy density lithium batteries^{1,2}. Among the several solid lithium ion conductors, a perovskite-related oxide in the (Li, La)TiO₃ system³ has attracted special attention in recent times^{4,5}. The ionic conducting phase is a nonstoichiometric oxide, $\text{La}_{2/3-x}\text{Li}_{3x}\square_{1/3-2x}\text{TiO}_3$ (\square = vacancy), which is stable over the composition range, $0.06 < x < 0.14$. The $x = 0.12$ member of this system exhibits a high lithium ion conductivity of $\sim 1.53 \times 10^{-3}$ S/cm at room temperature⁴. The structure of this material⁵ (figure 1) is typically that of a rhombohedral perovskite, consisting of TiO₆ octahedra slightly tilted along the rhombohedral axes with a Ti–O–Ti angle of 170°. The unique feature of this structure is the location of Li⁺ cations at 18*d* position (space group *R*–*3c*) in a square-planar oxygen coordination corresponding to the centre of every face of the pseudocubic perovskite structure. The low occupancy (1/6) of this site provides a continuously connected pathway for Li⁺ ion motion, giving rise to the high ionic conductivity.

A systematic consideration of the composition, structure and property of this material had enabled us to rationally design new lithium ion conductors, $\text{LiSr}_{1.65}\square_{0.35}\text{B}_{1.3}\text{B}'_{1.7}\text{O}_9$ (B = Ti, Zr; B' = Nb, Ta), exhibiting high conductivity of 0.11–0.12 S/cm at 360°C in the Ta oxides⁶. This composition, where La is replaced by Sr and part of Ti by Nb/Ta for charge compensation leaving a certain fraction of A sites vacant, is exactly analogous to the best lithium ion conducting composition in the (Li, La) TiO₃ system.

*For correspondence

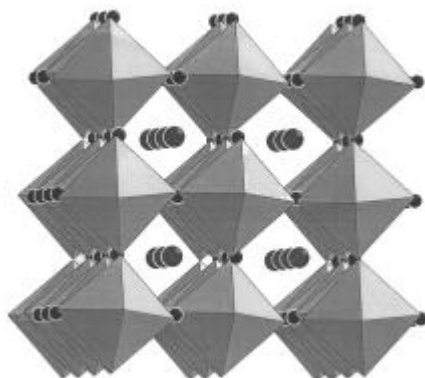


Figure 1. Structure of $\text{Li}_{0.5}\text{La}_{0.5}\text{TiO}_3$ (based on the data given in ref. 5).

In order to understand the influence of A site cations on the ionic conductivity of $\text{LiSr}_{1.65}\square_{0.35}\text{B}_{1.3}\text{B}'_{1.7}\text{O}_9$ ($\text{B} = \text{Ti, Zr}$; $\text{B}' = \text{Nb, Ta}$), we have investigated the substitution of Ca and Ba for Sr. This has generated new lithium ion conductors of composition, $\text{LiCa}_{1.65}\square_{0.35}\text{Ti}_{1.3}\text{B}'_{1.7}\text{O}_9$ ($\text{B} = \text{Nb, Ta}$). We have also investigated the possibility of having Ti^{4+} and W^{6+} instead of $\text{Ti}^{4+}/\text{Ta}^{5+}$ at the B site of the perovskite lattice. This has led to two new compositions with the perovskite structure, $\text{LiSr}_2\text{Ti}_{2.5}\text{W}_{0.5}\text{O}_9$ and $\text{LiSr}_{1.65}\square_{0.35}\text{Ti}_{2.15}\text{W}_{0.85}\text{O}_9$. In this paper, we describe the synthesis, characterization and lithium ion conductivity of the four new oxides, $\text{LiCa}_{1.65}\square_{0.35}\text{Ti}_{1.3}\text{B}'_{1.7}\text{O}_9$ ($\text{B} = \text{Nb, Ta}$), $\text{LiSr}_2\text{Ti}_{2.5}\text{W}_{0.5}\text{O}_9$ and $\text{LiSr}_{1.65}\square_{0.35}\text{Ti}_{2.15}\text{W}_{0.85}\text{O}_9$.

2. Experimental

$\text{LiCa}_{1.65}\square_{0.35}\text{Ti}_{1.3}\text{B}_{1.7}\text{O}_9$ ($\text{B} = \text{Nb, Ta}$) were prepared by reacting stoichiometric quantities of Li_2CO_3 , CaCO_3 , TiO_2 , and B_2O_5 ($\text{B} = \text{Nb, Ta}$) at 1100°C for 12 h. The mixture was then ground, pelletized and heated at 1200°C for 6 h and quenched to room temperature. A 10% excess of Li_2CO_3 was added to compensate the loss of lithia due to volatilization at higher temperatures. $\text{LiSr}_2\text{Ti}_{2.5}\text{W}_{0.5}\text{O}_9$ and $\text{LiSr}_{1.65}\square_{0.35}\text{Ti}_{2.15}\text{W}_{0.85}\text{O}_9$ were prepared from Li_2CO_3 , SrCO_3 , TiO_2 and WO_3 . The stoichiometric mixture of the starting materials was introduced into a furnace that was pre-heated to 1000°C . The temperature was then raised to 1200°C and held for 12 h. The materials were ground, pelletized and sintered again at 1200°C for 12 h and quenched. Pre-heating of the furnace and quenching were found to be essential for the formation of single-phase products. Powder X-ray diffraction patterns (XRD) were recorded on a Siemens D5005 X-ray diffractometer/Jeol JDX-8P X-ray diffractometer (CuK_α radiation) and unit cell parameters were obtained by least squares refinement of the powder XRD data.

Lithium ion conductivity was measured on sintered pellets coated with gold paste (cured at 600°C for 12 h) using HP 4194A impedance/gain phase analyser over the frequency range 100 Hz–15 MHz in the temperature range $30\text{--}800^\circ\text{C}$ in air. For each sample, measurements were made for both heating and cooling cycles. Samples were equilibrated at constant temperature for about 45 min prior to each impedance measurement. The conductivity was calculated from the low frequency intercept of the impedance plots.

3. Results and discussion

In table 1, we list the compositions, synthesis conditions and lattice parameters of $\text{LiCa}_{1.65}\square_{0.35}\text{Ti}_{1.3}\text{B}_{1.7}\text{O}_9$ (B = Nb, Ta) (**I**, **II**), $\text{LiSr}_2\text{Ti}_{2.5}\text{W}_{0.5}\text{O}_9$ (**III**) and $\text{LiSr}_{1.65}\square_{0.35}\text{Ti}_{2.15}\text{W}_{0.85}\text{O}_9$ (**IV**) along with their conductivity data. For comparison, we also give the corresponding data for $\text{LiSr}_{1.65}\square_{0.35}\text{Ti}_{1.3}\text{B}_{1.7}\text{O}_9$ (B = Nb, Ta) and $\text{Li}_{0.36}\text{La}_{0.55}\square_{0.09}\text{TiO}_3$

Table 1. Chemical composition, lattice parameter and lithium ion conductivity data for lithium-ion conducting perovskite oxides.

Composition	Synthesis conditions: (°C)/duration(h)	Lattice parameter (Å)	$S_{300^\circ\text{C}}$ (S/cm)	$S_{800^\circ\text{C}}$ (S/cm)	E_a (eV)
$\text{LiCa}_{1.65}\square_{0.35}\text{Ti}_{1.3}\text{Nb}_{1.7}\text{O}_9$ (I)	1100/12, 1200/6, 1250/6	a	1.0×10^{-5}	3.1×10^{-3}	0.71
$\text{LiCa}_{1.65}\square_{0.35}\text{Ti}_{1.3}\text{Ta}_{1.7}\text{O}_9$ (II)	1100/12, 1200/6, 1250/6	b	1.0×10^{-5}	4.2×10^{-3}	0.68
$\text{LiSr}_2\text{Ti}_{2.5}\text{W}_{0.5}\text{O}_9$ (III)	1200/(12 + 12)	3.925(1)	1.1×10^{-7}	1.0×10^{-4}	1.30
$\text{LiSr}_{1.65}\square_{0.35}\text{Ti}_{2.15}\text{W}_{0.85}\text{O}_9$ (IV)	1200/(12 + 12)	3.911(1)	1.6×10^{-4}	9.4×10^{-3}	0.49
$\text{LiSr}_{1.65}\square_{0.35}\text{Ti}_{1.3}\text{Nb}_{1.7}\text{O}_9^c$	1100/12, 1200/6	3.932(1)	4.2×10^{-2}	–	0.34
$\text{LiSr}_{1.65}\square_{0.35}\text{Ti}_{1.3}\text{Ta}_{1.7}\text{O}_9^c$	1100/12, 1250/6	3.932(1)	0.114	–	0.35
$\text{Li}_{0.36}\text{La}_{0.55}\square_{0.09}\text{TiO}_3^c$	650/2, 800/12, 1350/1	3.871(1)	0.130	–	0.33

^aOrthorhombic: $a = 5.363(1)$, $b = 5.464(1)$, $c = 7.662(3)$ Å. ^bOrthorhombic: $a = 5.363(1)$, $b = 5.456(1)$, $c = 7.661(1)$ Å; ^cData taken from [6, 7].

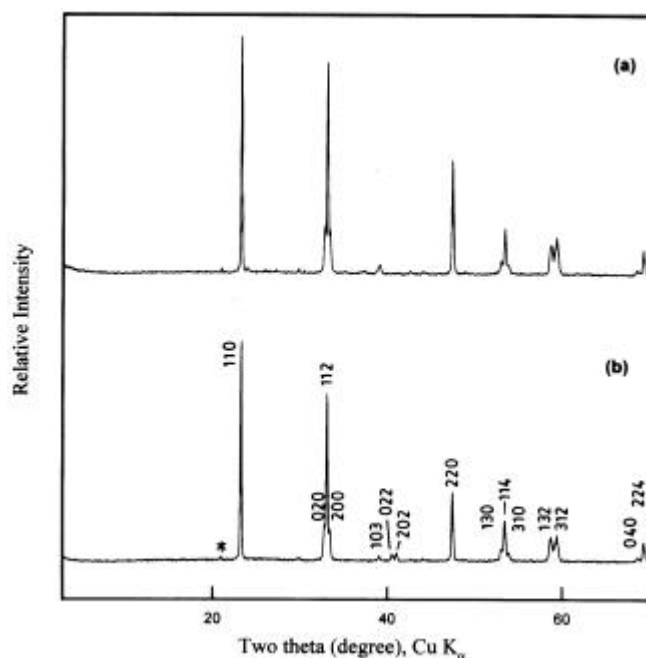


Figure 2. X-ray powder diffraction patterns of (a) $\text{LiCa}_{1.65}\square_{0.35}\text{Ti}_{1.3}\text{Nb}_{1.7}\text{O}_9$ and (b) $\text{LiCa}_{1.65}\square_{0.35}\text{Ti}_{1.3}\text{Ta}_{1.7}\text{O}_9$.

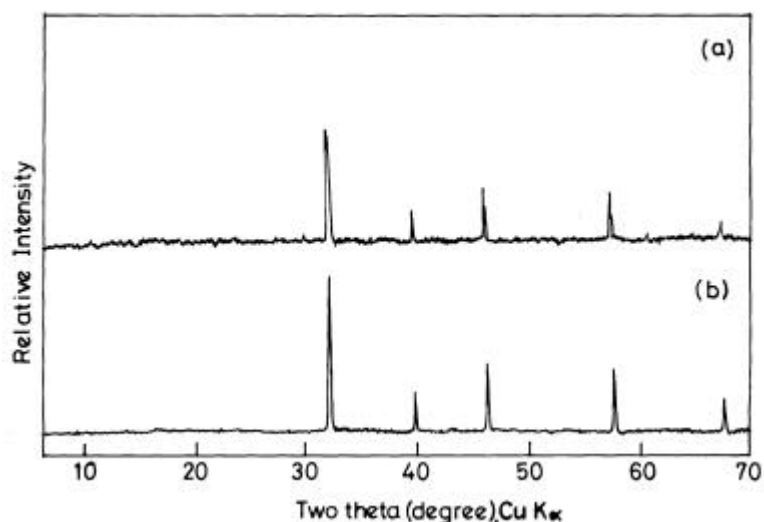


Figure 3. X-ray diffraction powder patterns of (a) $\text{LiSr}_{1.65}\square_{0.35}\text{Ti}_{215}\text{W}_{085}\text{O}_9$, and (b) $\text{LiSr}_2\text{Ti}_{2.5}\text{W}_{0.5}\text{O}_9$.

Table 2. The X-ray powder diffraction data for $\text{LiCa}_{1.65}\square_{0.35}\text{Ti}_{1.3}\text{Nb}_{1.7}\text{O}_9$.
 $a = 5.363(1)$, $b = 5.464(1)$, $c = 7.662(3)$ Å

h	k	l	d_{obs} (Å)	d_{cal} (Å)	I_{obs}
1	1	0	3.823	3.827	100
0	2	0	2.731	2.732	19
1	1	2	2.708	2.707	77
2	0	0	2.684	2.681	17
1	0	3	2.305	2.306	5
1	1	3	2.122	2.124	6
1	2	2	2.053	2.054	7
2	2	0	1.916	1.913	33
1	3	0	1.726	1.724	8
1	1	4	1.714	1.713	21
3	1	0	1.699	1.699	6
1	3	2	1.572	1.572	13
3	1	2	1.555	1.553	14
0	4	0	1.366	1.366	5
2	2	4	1.354	1.353	11
0	4	1	1.344	1.344	5

from the literature^{6,7}. Substitution of Ca for Sr resulted in the lowering of symmetry from cubic to orthorhombic as expected. The powder XRD patterns for **I** and **II** which are typical of orthorhombic GdFeO_3 -type structure are shown in figure 2. The patterns for **III** and **IV** (figure 3) shows cubic perovskite structure. The data for $\text{LiCa}_{1.65}\square_{0.35}\text{Ti}_{1.3}\text{Nb}_{1.7}\text{O}_9$ are indexed in table 2. Our attempts to prepare the corresponding Ba phase resulted in the formation of a mixture even after quenching from 1400°C.

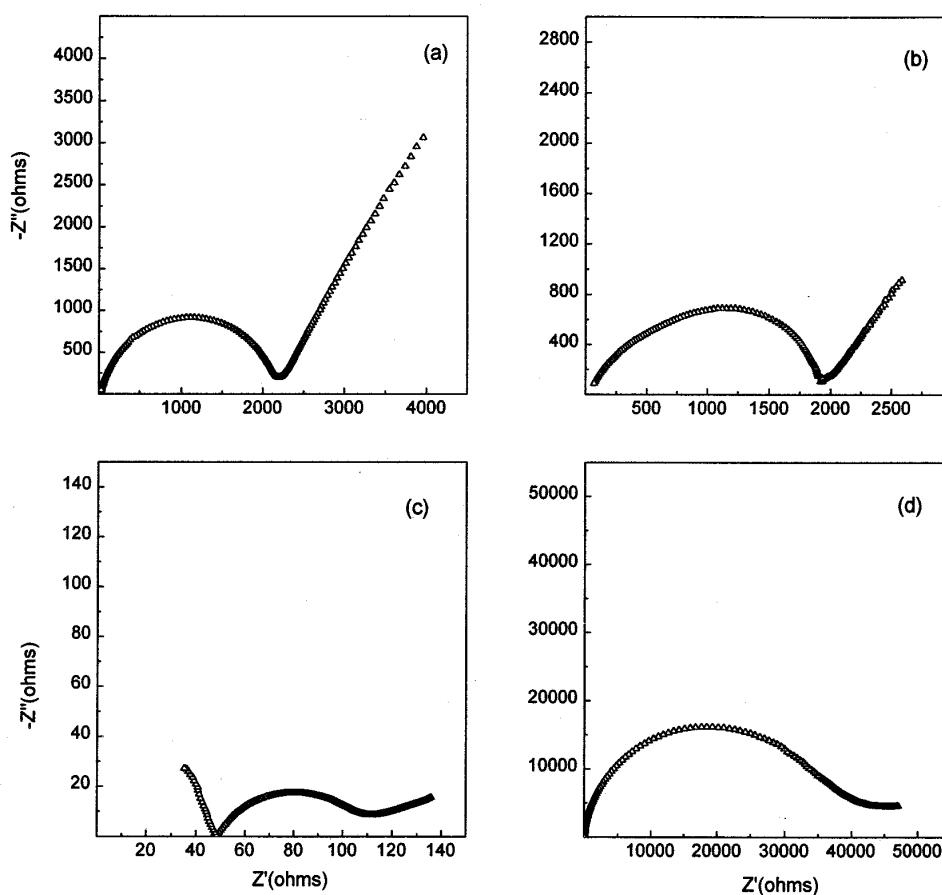


Figure 4. Typical a.c. impedance plots for (a) $\text{LiCa}_{1.65}\square_{0.35}\text{Ti}_{1.3}\text{Nb}_{1.7}\text{O}_9$ at 400°C , (b) $\text{LiCa}_{1.65}\square_{0.35}\text{Ti}_{1.3}\text{Ta}_{1.7}\text{O}_9$ at 400°C , (c) $\text{LiSr}_{1.65}\square_{0.35}\text{Ti}_{2.15}\text{W}_{0.85}\text{O}_9$ at 620°C and (d) $\text{LiSr}_2\text{Ti}_{2.5}\text{W}_{0.5}\text{O}_9$ at 620°C .

Ionic conductivity data for the perovskite oxides were obtained from a.c. impedance measurements. The typical impedance plots for $\text{LiCa}_{1.65}\square_{0.35}\text{Ti}_{1.3}\text{B}_{1.7}\text{O}_9$ ($\text{B} = \text{Nb}, \text{Ta}$) obtained at 400°C are shown in figure 4. The impedance plots for $\text{LiSr}_{1.65}\square_{0.35}\text{Ti}_{2.15}\text{W}_{0.85}\text{O}_9$ and $\text{LiSr}_2\text{Ti}_{2.5}\text{W}_{0.5}\text{O}_9$ at 620°C are also shown in figure 4.

Arrhenius plots for the conductivity of $\text{LiCa}_{1.65}\square_{0.35}\text{Ti}_{1.3}\text{B}_{1.7}\text{O}_9$ ($\text{B} = \text{Nb}, \text{Ta}$) are shown in figure 5. Conductivity (σ) values at 300°C and 800°C are listed in table 1 along with the activation energies (E_a). $\text{LiCa}_{1.65}\square_{0.35}\text{Ti}_{1.3}\text{Nb}_{1.7}\text{O}_9$ exhibits conductivity of $3.1 \times 10^{-3} \text{ S/cm}$ at 800°C with activation energy of 0.71 eV . From a comparison of the corresponding literature data (table 1), we see that substitution of Ca for Sr at the A site has resulted in a lowering of the conductivity. This could be due to the orthorhombic symmetry of the structure which would distort the 'bottleneck' for the lithium ion migration. For the cubic perovskite structure of the Sr analogue, the 'bottleneck' is a perfect square formed by four oxygens on (100) type planes. For the orthorhombic structure, the 'bottleneck' would necessarily distort to lower symmetry. Between the Nb and Ta members, the Ta member shows higher conductivity of $4.2 \times 10^{-3} \text{ S/cm}$ at 800°C

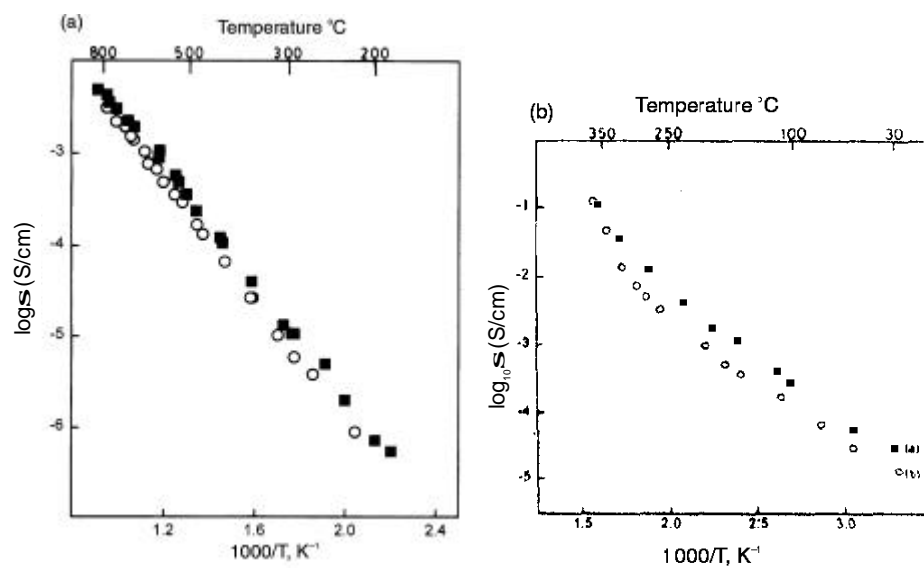


Figure 5. (a) Arrhenius plots for the ionic conductivity of: $\text{LiCa}_{1.65-0.35}\text{Ti}_{1.3}\text{Nb}_{1.7}\text{O}_9$ (O) and $\text{LiCa}_{1.65-0.35}\text{Ti}_{1.3}\text{Ta}_{1.7}\text{O}_9$ (■). (b) Data for $\text{LiSr}_{1.65-0.35}\text{Ti}_{1.3}\text{Ta}_{1.7}\text{O}_9$ (■) and $\text{LiSr}_{1.65-0.35}\text{Zr}_{1.3}\text{Ta}_{1.7}\text{O}_9$ (O) taken from ref. 6.

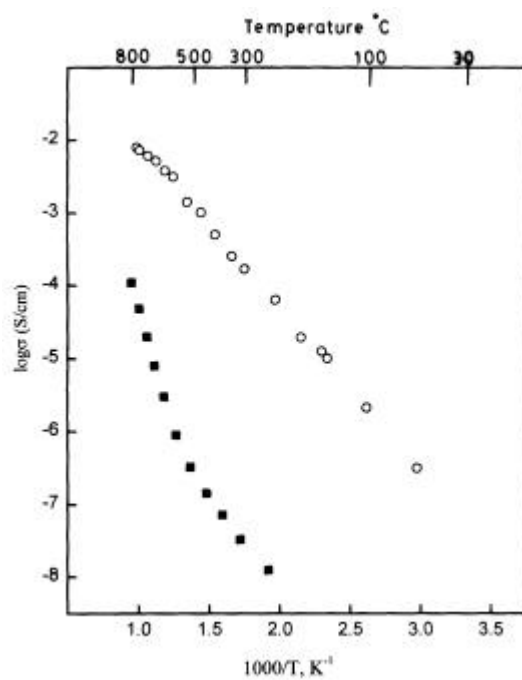


Figure 6. Arrhenius plots for the ionic conductivity of $\text{LiSr}_{1.65-0.35}\text{Ti}_{2.15}\text{W}_{0.85}\text{O}_9$ (O) and $\text{LiSr}_2\text{Ti}_{2.5}\text{W}_{0.5}\text{O}_9$ (■).

($E_a = 0.68$ eV). A similar difference in conductivity between Nb and Ta members has been observed in the corresponding Sr analogues⁶. The difference has been attributed to the smaller distortion of the TaO₆ octahedra as compared to the NbO₆ octahedra. Since the HOMO–LUMO gap between oxygen 2p and the metal d^0 states of Nb/Ta would be larger for Ta than for Nb oxide, the TaO₆ octahedra will be less distorted than NbO₆ octahedra⁸. Less distorted TaO₆ octahedra would provide smoother potential for the migration of Li⁺ ions.

The Arrhenius plots for the conductivity of LiSr₂Ti_{2.5}W_{0.5}O₉ (**III**) and LiSr_{1.65}□_{0.35}Ti_{2.15}W_{0.85}O₉ (**IV**) are given in figure 6. We see that phase **IV** shows a higher conductivity than phase **III**, revealing the importance of A site vacancies for lithium ion conduction. For example, while **III** shows conductivity of 1×10^{-4} S/cm at 800°C, **IV** exhibits higher conductivity of 9.4×10^{-3} S/cm at the same temperature. One would expect introduction of W⁶⁺ to give higher conductivity than the corresponding Nb⁵⁺/Ta⁵⁺ analogues (other things being equal) because of the higher covalency of W–O bonds with respect to the Nb–O/Ta–O bonds. On the other hand, Nb/Ta compounds show a higher conductivity. The results therefore suggest that the larger formal charge on W⁶⁺ as compared to Nb⁵⁺/Ta⁵⁺/Ti⁴⁺ likely provides deeper potential wells for Li⁺ ion migration and hence the lower conductivity.

4. Conclusion

Based on structure-property correlations of the well-known lithium ion conductor in the (Li, La)TiO₃ system, we have synthesized four new perovskite oxides in the Li–Ca/Sr–Ti/Nb/Ta/W–O systems that exhibit significant lithium-ion conduction at elevated temperatures. The present work reveals the importance of structural distortion associated with A-site cation size, vacancies at A-site and the difference in formal charge between B-site cations, on the lithium-ion conductivity of this family of oxides.

Acknowledgements

We thank the Department of Science and Technology, Government of India, for financial support. LS thanks the Council of Scientific and Industrial Research, New Delhi for a fellowship. We also thank Dr. K Ramesha for his help in the synthesis.

References

1. Robertson A D, West A R and Ritchie A G 1997 *Solid State Ionics* **104** 1
2. Gopalakrishnan J, Shukla A K and Thangadurai V 1999 *Curr. Sci.* **76** 1473
3. Belous A G, Novitskaya G N, Polyanetskaya S V and Gornikov Yu I 1987 *Izv. Akad. Nauk SSSR, Neorg. Mater.* **23** 470
4. Fourquet J L, Duroy H and Crosnier-Lopez M P 1996 *J. Solid State Chem.* **127** 283
5. Alonso J A, Sanz J, Santamaría J, León C, Várez A and Fernández-Díaz M T 2000 *Angew. Chem., Int. Ed. Engl.* **39** 619
6. Thangadurai V, Shukla A K and Gopalakrishnan J 1999 *Chem. Mater.* **11** 835
7. Inaguma Y, Liqun C, Itoh M, Nakamura T, Uchida T, Ikuta H and Wakihara M 1993 *Solid State Commun.* **86** 689
8. Bhuvanesh N S P and Gopalakrishnan J 1997 *J. Mater. Chem.* **7** 2297